

Global Mapping Function (GMF): A new empirical mapping function based on numerical weather model data

J. Boehm,¹ A. Niell,¹ P. Tregoning,¹ and H. Schuh¹

Received 20 December 2005; revised 23 January 2006; accepted 10 February 2006; published XX Month 2006.

[1] Troposphere mapping functions are used in the analyses of Global Positioning System and Very Long Baseline Interferometry observations to map a priori zenith hydrostatic and wet delays to any elevation angle. Most analysts use the Niell Mapping Function (NMF) whose coefficients are determined from site coordinates and the day of year. Here we present the Global Mapping Function (GMF), based on data from the global ECMWF numerical weather model. The coefficients of the GMF were obtained from an expansion of the Vienna Mapping Function (VMF1) parameters into spherical harmonics on a global grid. Similar to NMF, the values of the coefficients require only the station coordinates and the day of year as input parameters. Compared to the 6-hourly values of the VMF1 a slight degradation in short-term precision occurs using the empirical GMF. However, the regional height biases and annual errors of NMF are significantly reduced with GMF. **Citation:** Boehm, J., A. Niell, P. Tregoning, and H. Schuh (2006), Global Mapping Function (GMF): A new empirical mapping function based on numerical weather model data, *Geophys. Res. Lett.*, 33, LXXXXX, doi:10.1029/2005GL025546.

1. Introduction

[2] For space geodetic measurements, estimates of atmosphere delays are highly correlated with site coordinates and receiver clock biases. Thus it is important to use the most accurate models for the atmosphere delay to reduce errors in the estimates of the other parameters. Numerical Weather Models (NWM) provide the spatial distribution of refractivity throughout the troposphere with high temporal resolution for mapping the zenith troposphere delay to the elevation of each observation by so-called mapping functions. The information needed for the mapping functions must be obtained from an external source, i.e., the NWM, prior to geodetic data analysis. In contrast, the Niell Mapping Function (NMF) was built on one year of radiosonde profiles from the northern hemisphere [Niell, 1996]; the spatial and temporal variability of the mapping function is accounted for with only a latitude and seasonal dependence. This empirical approach considerably simplifies the estimation process since no external data are required. However, following the development of NMF, two deficiencies became evident: a) latitude-dependent biases, which are largest in high southern latitudes, and b) the lack of sensitivity to the longitude of a site, what causes systematic distortions of estimated positions in some areas, for example over northeast China and Japan. The simple

temporal and latitudinal functions of the NMF do not provide the resolution to capture the higher variability in space and time that are seen in mapping functions based on NWM data [Boehm and Schuh, 2004; Boehm et al., 2006].

[3] Boehm et al. [2006] showed from an analysis of Very Long Baseline Interferometry (VLBI) observations that the application of the Vienna Mapping Function (VMF1), with coefficients given at 6-hourly time intervals, considerably improves the precision of geodetic results such as baseline lengths and station heights. VMF1 is currently the mapping function providing globally the most accurate and reliable geodetic results. Moreover, systematic station height changes of up to 10 mm occur when changing from the NMF to the VMF1.

[4] The goal of this paper is to present a mapping function which can be used globally and implemented easily in existing geodetic analysis software and which provides consistency with NWM-based mapping functions, in particular with the VMF1 [Boehm et al., 2006]. The parameterization of the coefficients in the three-term continued fraction (see equation (1)) that is used in most mapping functions has been refined to include a dependence on longitude. The accuracies of the mapping functions have been improved by extending the temporal range of input data used and also by global sampling of the atmosphere by raytracing through a global NWM instead of the limited number of radiosonde sites used to derive the NMF. The resulting mapping functions, one each for the hydrostatic and wet components, are designated the Global Mapping Function (GMF). We compare the empirical GMF with mapping functions derived from radiosonde data, with NMF, and with VMF1.

2. Mapping Functions

[5] For space geodetic measurements it is convenient to characterize the azimuthally symmetric component of the atmospheric delay with a value in the zenith direction that varies with time on a scale of twenty minutes to a few hours. The delay in the direction of an observation is related to the zenith delay by a mapping function, which is modelled with sufficient accuracy for elevations down to 3° using a three term continued fraction in $\sin e$ elevation, e [Niell, 1996] given by:

$$mf(e) = \frac{1 + \frac{a}{1 + \frac{b}{1 + c}}}{\sin e + \frac{a}{\sin e + \frac{b}{\sin e + c}}} \quad (1)$$

The parameters a , b , and c are different for the hydrostatic and wet components of the atmosphere designated with indices h or w in section 3. They should be related with

¹Institute of Geodesy and Geophysics, Vienna, Austria.

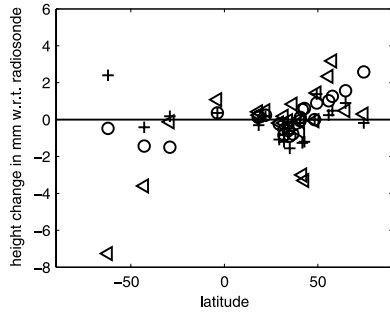


Figure 1. Mean height differences in mm for hydrostatic NMF (triangles), GMF (pluses), and VMF1 (circles) relative to radiosonde based mapping functions for 1992.

100 sufficient accuracy to the characteristics of the atmosphere
 101 at the time of observation to avoid introducing significant
 102 error into the estimation of the geodetic site coordinates. For
 103 NMF [Niell, 1996], each of the parameters is a constant or a
 104 function of site latitude (symmetric about the equator) and
 105 day of year. Thus, only the seasonal dependence of the
 106 temporal variation of the atmosphere is taken into account.
 107 The mapping functions IMF [Niell, 2001] and VMF1
 108 [Boehm et al., 2006] use the output of a numerical weather
 109 analysis to provide information specifically for the geo-
 110 graphic location of the site with a temporal resolution of six
 111 hours. They differ in the ease of computation of the
 112 parameters and the amount of data used from the NWM.
 113 While VMF1 is more accurate, IMF is more generally
 114 applicable. The accuracy improvement over NMF is
 115 especially significant for the hydrostatic component for
 116 both VMF1 and IMF.

117 [6] Different mapping functions produce different coordi-
 118 nate estimates, not only in terms of precision and repeat-
 119 ability but also with different biases and seasonal variability.
 120 It is necessary to use consistent mapping functions for all
 121 analyses in order to derive consistent sets of coordinates.
 122 The VMF1 is provided only at discrete locations, for
 123 example, all IVS (International VLBI Service for Geodesy
 124 and Astrometry) sites and all IGS (International GNSS
 125 Service) sites, and does not cover the whole time period
 126 of global GPS observations since the early 1990s. There-
 127 fore, it is desirable to have a mapping function compatible
 128 with NMF, that can be computed empirically for any site at
 129 any date but which is more consistent with the VMF1 than
 130 is NMF. Such a mapping function could be seen as a back-
 131 up in case the NWM-based models are not available for
 132 some period of time or are discontinued.

133 3. Determination of the Global Mapping 134 Function (GMF)

135 [7] Using $15^\circ \times 15^\circ$ global grids of monthly mean
 136 profiles for pressure, temperature, and humidity from the
 137 ECMWF (European Centre for Medium-Range Weather
 138 Forecasts) 40 years reanalysis data (ERA40), the coeffi-
 139 cients a_h and a_w were determined for the period September
 140 1999 to August 2002 applying the same strategy which was
 141 used for VMF1. Taking empirical equations for b and c
 142 (from VMF1) the parameters a were derived by a single
 143 raytrace at 3.3° initial elevation angle [Boehm et al., 2006].

Thus, at each of the 312 grid points, 36 monthly values
 144 were obtained for the hydrostatic and wet a parameters. The
 145 hydrostatic coefficients were reduced to mean sea level by
 146 applying the height correction given by Niell [1996]. The
 147 mean values, a_0 , and the annual amplitudes A of a sinusoi-
 148 dal function (equation (2)) were fitted to the time series of
 149 the a parameters at each grid point, with the phases referred
 150 to January 28, corresponding to the NMF. The standard
 151 deviations of the monthly values at the single grid points
 152 with respect to equation (2) increase toward higher latitude
 153 from the equator, with a maximum value of 8 mm (equiv-
 154 alent station height error) in Siberia. For the wet component,
 155 the standard deviations are smaller with maximum values of
 156 about 3 mm at the equator. 157

$$a = a_0 + A \cdot \cos\left(\frac{\text{doy} - 28}{365} \cdot 2\pi\right) \quad (2)$$

$$a_0 = \sum_{n=0}^9 \sum_{m=0}^n P_{nm}(\sin \varphi) \cdot [A_{nm} \cdot \cos(m \cdot \lambda) + B_{nm} \cdot \sin(m \cdot \lambda)] \quad (3)$$

Then, the global grid of the mean values a_0 and that of the
 161 amplitudes A for both the hydrostatic and wet coefficients of
 162 the continued fraction form were expanded into spatial
 163 spherical harmonic coefficients up to degree and order 9
 164 (according to equation (3) for a_0) in a least-squares
 165 adjustment. The residuals of the global grid of a_0 and A
 166 values to the spherical harmonics are in the sub-millimeter
 167 range (in terms of station height). The hydrostatic and wet
 168 coefficients a for any site coordinates and day of year can
 169 then be determined using equation (2). 170

4. Validation and Comparison of Mapping Functions

4.1. Validation of Mapping Functions With Radiosondes

[8] The most accurate computation of azimuthally sym-
 175 metric mapping functions is assumed to be obtained from
 176 vertical profiles of temperature, pressure, and humidity from
 177 radiosondes [Niell et al., 2001]. The mapping function is
 178 then computed as the ratio of the delay (obtained by
 179 raytracing) along the path at the desired elevation to the
 180 delay in the zenith direction. For convenience we compare 181

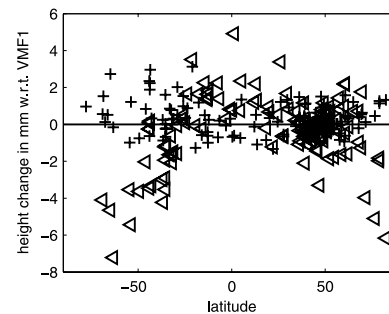


Figure 2. Mean height changes in mm when using NMF (triangles) and GMF (pluses) in GPS analysis with heights obtained with VMF1 as reference.

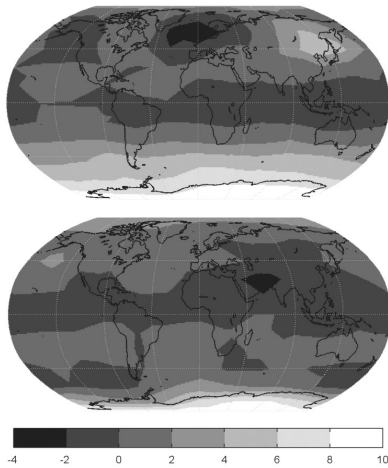


Figure 3. Mean height changes (in mm) when using the hydrostatic GMF instead of NMF for (top) January and (bottom) July determined by applying the rule of thumb. The largest differences can be found in January south of 45°S and in northeast China and Japan, with station height differences up to 10 mm.

182 the mapping functions for a vacuum (outgoing) elevation
 183 angle of 5°. The radiosonde data used for this comparison
 184 are from 23 sites and span the latitude range from -66° to
 185 +75°. However, it has to be mentioned that the majority of
 186 the radiosonde sites are in the northern hemisphere. A ‘rule
 187 of thumb’ [MacMillan and Ma, 1994] states that for
 188 azimuthally symmetric delay errors and observations down
 189 to approximately 5°, the height error is approximately one
 190 fifth of the delay error at the lowest elevation. The mapping
 191 function differences have been converted to an equivalent
 192 height difference using this rule of thumb because station
 193 height changes are more easily visualized than differences
 194 in the a coefficients. The mean station height differences,
 195 averaged over the year, are shown in Figure 1 after
 196 comparing the hydrostatic delays from NMF, GMF, and
 197 VMF1 with radiosonde data. The most important feature is
 198 the significantly smaller bias for hydrostatic GMF compared
 199 to hydrostatic NMF, thus confirming that the mean biases
 200 can be reduced with GMF. On the other hand, GMF and
 201 NMF are not significantly different with respect to the
 202 standard deviations of the height changes (not shown here)
 203 since both contain only annual time variability, whereas the
 204 actual variations occur on weekly, daily, and sub-daily time
 205 scales. The influence of the wet mapping functions is less
 206 critical than the hydrostatic component in GPS and VLBI
 207 analyses, since the wet delays are typically smaller than the
 208 hydrostatic delays by a factor of 10.

209 4.2. NMF and GMF Compared to VMF1 in 210 GPS Analysis

211 [9] A global network of more than 100 GPS stations was
 212 analysed with the software package GAMIT Version 10.21
 213 [King and Bock, 2005; Herring, 2005] applying the NMF,
 214 GMF, and VMF1 mapping functions. We processed obser-
 215 vations from July 2004 through June 2005, producing a
 216 fiducial-free global network for each day. The elevation
 217 cutoff angle was set to 7° and no downweighting of low
 218 observations was applied to make the performance of the

mapping functions most visible. Atmospheric pressure 219
 loading (tidal and non-tidal) [Tregoning and van Dam, 220
 2005] was applied along with ocean tide loading and the 221
 IERS2003 solid Earth tide model [McCarthy and Petit, 222
 2004]. We estimated satellite orbital parameters, station 223
 coordinates, zenith tropospheric delay parameters every 224
 2 hours, and resolved ambiguities where possible. We 225
 used ~60 sites to transform the fiducial-free networks 226
 into the ITRF2000 by estimating 6-parameter transforma- 227
 tions (3 rotations, 3 translations) [Herring, 2005]. For the 228
 investigations described below the time series were used 229
 of those 133 stations which have more than 300 daily 230
 height estimates. The latitudes of the sites are indicated in 231
 Figure 2 which shows the mean changes of GPS station 232
 heights with NMF or GMF relative to using VMF1. It is 233
 evident that the agreement between VMF1 and GMF is very 234
 good, whereas station height differences up to 10 mm occur 235
 in the southern hemisphere south of 45°S and in the Japan 236
 region when changing from VMF1 to NMF. 237

238 4.3. NMF Versus GMF

[10] Computing hydrostatic GMF and NMF for each 239
 month on a global grid and applying the rule of thumb, 240
 we derived corresponding station height differences. In 241
 Figure 3 the height changes from NMF to GMF are plotted 242
 for January and July. These comparisons show that there is 243
 pretty good agreement between NMF and GMF in July 244
 (apart from Antarctica), but that in January differences are 245
 large (up to 15 mm) south of 45°S and in northeast China 246
 and Japan. These height changes vary throughout the year 247
 and influence other parameters such as scale and geocenter 248
 motion. 249

[11] In Figure 4 the three hydrostatic mapping functions 250
 discussed in this paper at 5° elevation are plotted for 251
 Fortaleza, Brazil. The NMF does not show a seasonal 252
 variation because this station is situated near the equator 253
 (2°S). In contrast, the GMF reflects a seasonal variability 254
 and, on average, agrees much better with the VMF1. 255
 However, a deficiency is evident in both empirical mapping 256
 functions compared to the VMF1 because neither NMF 257
 nor GMF reveal the unusual meteorological conditions 258

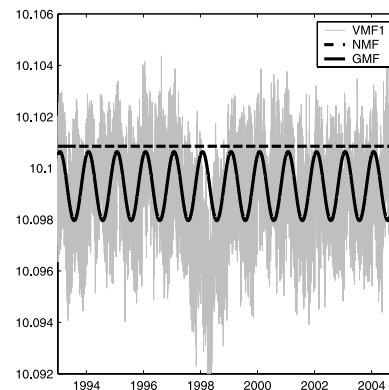


Figure 4. Hydrostatic mapping function at 5° elevation at Fortaleza, Brazil. Phenomena such as the El Niño event in 1997 and 1998 cannot be accounted for with empirical mapping functions like NMF or GMF that contain only average seasonal terms.

259 described by the VMF1 during the El Niño phenomena in
260 1997 and 1998.

262 5. Conclusions

263 [12] To achieve the highest accuracy in VLBI and GPS
264 analyses, it is recommended to use troposphere mapping
265 functions that are based on data from numerical weather
266 models. Today, these mapping functions (e.g., VMF1
267 [Boehm et al., 2006] or IMF [Niell, 2001]) are available
268 as time series of coefficients with a resolution of six hours.
269 However, for particular time periods or stations where
270 NWM-based mapping functions are not available, the
271 GMF can be used without introducing systematic biases
272 in the coordinate time series, although the short-term
273 precision will suffer compared to the VMF1. The GMF
274 can serve as a ‘back-up’ mapping function or a compatible
275 empirical representation of the more complex NWM-based
276 mapping functions. The GMF provides better precision than
277 the NMF and smaller height biases with respect to VMF1. It
278 can be implemented very easily because it uses the same
279 input parameters (station coordinates and day of year) as
280 NMF, which is already implemented in most space geodesy
281 software packages. Code for *FORTRAN* implementations of
282 VMF1 and GMF are provided at [http://www.hg.tuwien.](http://www.hg.tuwien.ac.at/~ecmwf1)
283 [ac.at/~ecmwf1](http://www.hg.tuwien.ac.at/~ecmwf1), as are the input data for VMF1 and IMF.

284 [13] **Acknowledgments.** We would like to thank the Zentralanstalt
285 fuer Meteorologie und Geodynamik (ZAMG) for allowing us access to the
286 data of the European Centre for Medium-Range Weather Forecasts
287 (ECMWF). Johannes Boehm and Harald Schuh are grateful to the Austrian
288 Science Fund (FWF) for supporting this work under project P16992-N10.

Arthur Niell was supported by NASA contract NNG05HY03C. The GPS 289
analyses were computed on the Terrawulf linux cluster belonging to the 290
Centre for Advanced Data Inference at the Research School of Earth 291
Sciences, the Australian National University. 292

References 293

- Boehm, J., and H. Schuh (2004), Vienna mapping functions in VLBI ana- 294
lyses, *Geophys. Res. Lett.*, *31*, L01603, doi:10.1029/2003GL018984. 295
- Boehm, J., B. Werl, and H. Schuh (2006), Troposphere mapping functions 296
for GPS and very long baseline interferometry from European Centre for
Medium-Range Weather Forecasts operational analysis data, *J. Geophys.* 297
Res., *111*, B02406, doi:10.1029/2005JB003629. 298
- Herring, T. A. (2005), GLOBK global Kalman filter VLBI and GPS ana- 300
lysis program, version 10.1, Mass. Inst. of Technol., Cambridge. 301
- King, R. W., and Y. Bock (2005), Documentation for the GAMIT GPS 302
processing software release 10.2, Mass. Inst. of Technol., Cambridge. 303
- MacMillan, D. S., and C. Ma (1994), Evaluation of very long baseline 304
interferometry atmospheric modeling improvements, *J. Geophys. Res.*, 305
99, 637–652. 306
- McCarthy, D. D., and G. Petit (Eds.) (2004), IERS conventions (2003), 307
IERS Tech. Note 32, Verl. des Bundesamtes für Kartogr. und Geod., 308
Frankfurt am Main, Germany. 309
- Niell, A. E. (1996), Global mapping functions for the atmosphere delay at 310
radio wavelengths, *J. Geophys. Res.*, *101*, 3227–3246. 311
- Niell, A. E. (2001), Preliminary evaluation of atmospheric mapping func- 312
tions based on numerical weather models, *Phys. Chem. Earth*, *26*, 475– 313
480. 314
- Niell, A. E., A. J. Coster, F. S. Solheim, V. B. Mendes, P. C. Toor, R. B. 315
Langley, and C. A. Upham (2001), Comparison of measurements of 316
atmospheric wet delay by radiosonde, water vapor radiometer, GPS, 317
and VLBI, *J. Atmos. Oceanic Technol.*, *18*, 830–850. 318
- Tregoning, P., and T. van Dam (2005), Atmospheric pressure loading 319
corrections applied to GPS data at the observation level, *Geophys.* 320
Res. Lett., *32*, L22310, doi:10.1029/2005GL024104. 321
- J. Boehm, A. Niell, H. Schuh, and P. Tregoning, Institute of Geodesy and 323
Geophysics, Gusshausstrasse 27–29, A-1040 Vienna, Austria. (johannes. 324
boehm@tuwien.ac.at) 325